Journal of Molecular Catalysis A: Chemical 286 (2008) 128–136

Contents lists available at ScienceDirect

Journal of Molecular Catalysis A: Chemical

journal homepage: www.elsevier.com/locate/molcata

Quantum chemical modelling of the C–H cleavage mechanism in oxidation of ethylbenzene and its derivates by ethylbenzene dehydrogenase

Maciej Szaleniec[a,*], Malgorzata Witko[a], Johann Heider[b]

[a] Institute of Catalysis and Surface Chemistry, Polish Academy of Sciences, Niezapominajek 8, 30-239 Krakow, Poland
[b] Institut für Biologie, Technische Universität Darmstadt, Germany

ARTICLE INFO

Article history:
Received 30 October 2007
Received in revised form 14 February 2008
Accepted 20 February 2008
Available online 4 March 2008

Keywords:
Ethylbenzene dehydrogenase
Quantitative structure activity relationship (QSAR)
DFT

ABSTRACT

Ethylbenzene dehydrogenase is an enzyme capable of oxygen-independent stereospecific oxidation of ethylbenzene to (*S*)-1-phenylethanol. Moreover, it oxidises a wide range of other alkylaromatic and alkyl-heterocylic compounds. In oxidation processes the C–H bond cleavage is supposed to be a rate-limiting step that may proceed either via a radical or a carbocation intermediate. The reaction rate can also be under control of energy barrier of OH rebound to the activated hydrocarbon proceeding also according to radical or carbocation mechanism.

In order to assess the probabilities of the two alternative mechanisms, the Gibbs free energies of formation of both radical and carbocation intermediates from various substrates are determined by quantum chemical calculations on DFT level. It is found that the obtained thermodynamic parameters $\Delta G^{\text{radical}}$ and $\Delta G^{\text{carbocation}}$ correlate with widely accepted molecular descriptors such as radical Yamamoto–Otsu E_r ($R^2 = 0.70$) and Hammett σ^+ values ($R^2 = 0.91$).

The effects of modification of substrate structures on the stabilization of radical/carbocation intermediate (as approximation of transition state) are correlated with enzyme kinetic results. None correlation is apparently satisfactory, but taking into account the distribution of scattered points, the carbocation intermediate seems to be (on average) more probable than a free radical intermediate. In addition, a simple QSAR model describing all characterized substrates is obtained taking into consideration only two parameters, $\Delta\Delta G$ of carbocation formation and molecular refractivity (MR) as a measure of steric hindrance.

1. Introduction

Mononuclear molybdenum enzymes constitute a class of biocatalysts that contain the molybdenum cofactor in their active centres. The cofactor consists of one Mo atom ligated to one or two molybdopterins. The recently discovered ethylbenzene dehydrogenase (EBDH), which is molybdoenzyme belonging to the DMSO reductase family [1], catalyzes the molecular oxygen-independent, stereospecific hydroxylation of ethylbenzene to (*S*)-1-phenylethanol. It is the first known enzyme capable of direct anaerobic oxidation of a non-activated hydrocarbon [1–4] (Fig. 1).

EBDH promises potential applications in fine chemical and pharmaceutical industries owing to the following facts: (i) pure enantiomers of alcohols are valuable as building blocks for physiologically active compounds, e.g. 1-phenylethanol itself is used as food and drink flavouring agent and additive of cosmetics [5,6] and (ii) EBDH reacts with a relatively broad spectrum of alkyl substituted aromatic and heterocyclic compounds [7,8] (Fig. 2). Therefore, it should be applicable in producing a wide range of chiral alcohols that might find industrial application.

The principal mechanism of ethylbenzene oxidation at the molybdenum cofactor of EBDH is shown in Fig. 3. First, one of the C–H bonds of the methylene group must be cleaved in order to activate the hydrocarbon. This step may proceed hetero- (Fig. 3a) or homolytically (Fig. 3b), which implies transition state (TS1) of either a carbocation or a radical character, respectively. Subsequently, an OH ligand present in the active centre must be shuttled back toward the activated (radical or carbocation) hydrocarbon intermediate. The second transition state (TS2) would therefore constitute either a reaction of two radicals (hydroxyl and hydrocarbonyl) or a reaction of a negatively charged OH^- and a carbocation. Because each of these two scenarios has serious drawbacks, also a "mixed" model, which begins with a homolytic cleavage of the C–H bond leading to a radical intermediate (Fig. 3c) should be considered. In such a mechanism a second electron transfer from the radical intermediate to the Mo cofactor may occur, creating a carbocation intermediate and a hydroxy-anion bound to the active site, whose subsequent reaction forms the final product. Therefore, both

* Corresponding author. Tel.: +48 12 6395 157; fax: +48 12 4251923.
E-mail address: ncszalen@cyf-kr.edu.pl (M. Szaleniec).

1381-1169/$ – see front matter © 2008 Elsevier B.V. All rights reserved.
doi:10.1016/j.molcata.2008.02.016

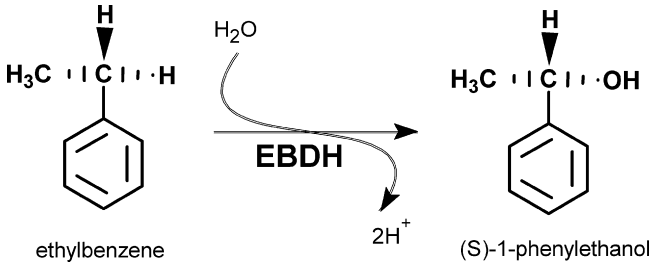

Fig. 1. The reaction scheme of ethylbenzene oxidation by EBDH.

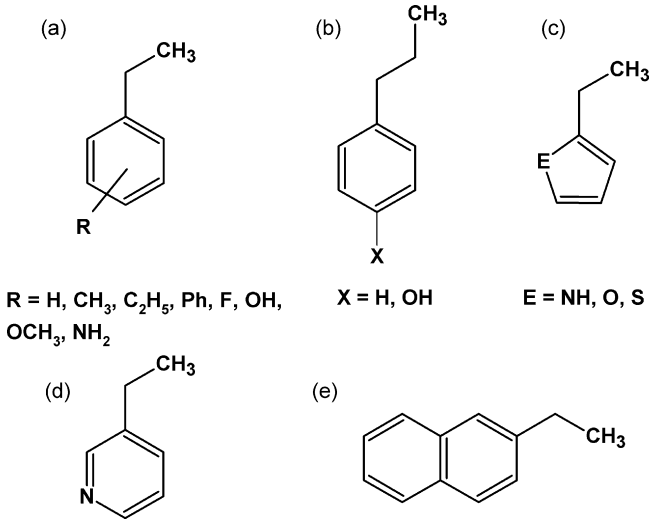

Fig. 2. Molecular structures of some ethylbenzene dehydrogenase substrates: (a) ethylbenzene and its derivates (b) *n*-propylbenzene and its derivate, (c) five member ring ethyl heterocycles (d) 3-ethylpyridine and (e) 2-ethylnaphtalene.

transition state barriers might be rate limiting and both may either involve radical or carbocation species. Moreover, one can imagine that transfer process of the second electron is also associated with some kind of energetic barrier.

Quantitative structure activity relationship (QSAR) analysis may help in evaluating the above mechanisms by careful breaking down of kinetic results for a series of substrates. However, appropriate descriptors for the expected intermediates for standard QSAR analysis are not available for many of the EBDH substrates. Therefore, QSAR analysis does not provide unequivocal answer to the question, whether the rate-limiting step of the EBDH reaction proceeds via free radicals or carbocations. In the description of kinetics of reactions involving carbocation intermediates, usually the Hammett σ^+ constant is applied as a parameter describing electronic effects of substituents, which change the strong resonance coupling of the reaction site with a conjugated or aromatic system [9]. However, similar correlations of σ^+ with the reaction kinetics are also known from radical reactions [10]. Therefore, one needs a method to compare stabilization effects introduced by various substituents into radical/carbocation intermediate (as an approximation of the transition state) in a similar, comparable manner, which would allow quantitative analysis of kinetic data. As a result, simple gas-phase quantum chemical calculations are undertaken for a range of enzyme substrates, which yield changes of thermochemical functions of free radical and carbocation formations. The performed calculations allow establishing a correlation between differences in the obtained gas-phase $\Delta G^{\#}$ and the observed experimental kinetic results for 21 different substrates and provide clues for understanding the reaction mechanism. The aim of this paper is to introduce a useful methodology of correlation analysis based on thermodynamic parameters derived from theoretical calculation. It is a strong belief that such an approach can significantly broaden the applicability of transitional QSAR analysis.

2. Experimental

2.1. Kinetic tests

Enzyme activity was routinely determined as described previously [7,8]. To assess for variations in enzyme activities of different batches, measurements were referred to standard tests with ethylbenzene (standard assay conditions, 60 μM ethylbenzene concentration). The reaction rates with ethylbenzene in standard conditions were set as 100%.

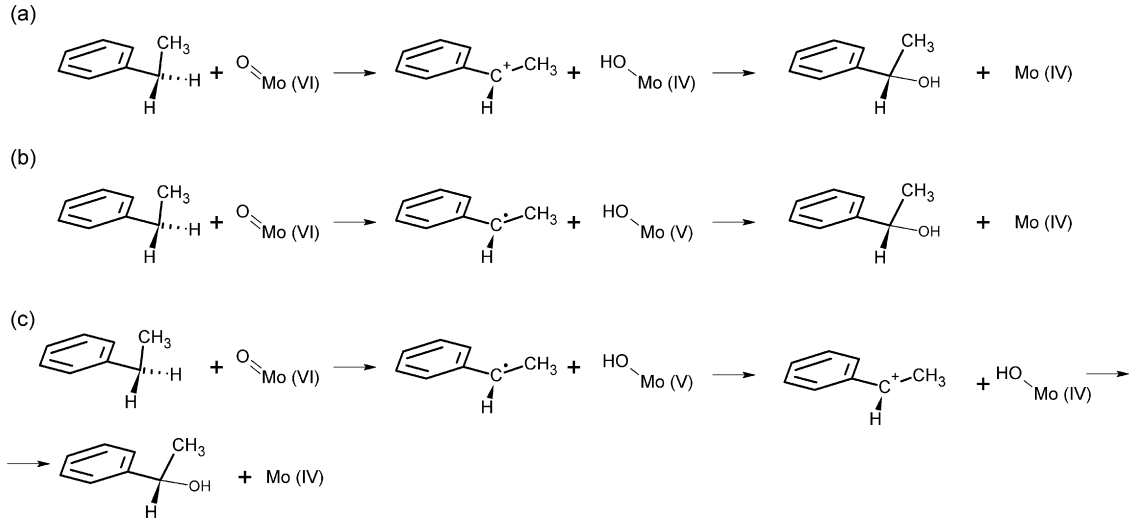

Fig. 3. Hypothetical variants of reaction mechanism catalyzed by EBDH: (a) heterolytic C–H cleavage (TS1) by carbocation formation and formation of the alcohol (TS2) by transfer of a hydroxide ion; (b) homolytic cleavage of the C–H bond leading to a radical intermediate and formation of product by transfer of a hydroxyl radical equivalent; (c) 'mixed' mechanism comprising of hemolytic cleavage of C–H bond and then electron transfer yielding carbocation species and Mo(IV) and finally resulting in the formation of product by transfer of hydroxide ion.

2.2. Quantum chemical modelling

Quantum chemical calculations were performed for 21 EBDH substrates and for a range of additional ethylbenzene derivates that were used in correlation analysis and method validation. All calculations were conducted in the Gaussian 03 suite of programs [11]. The electron correlation and exchange were described by the B3LYP exchange-correlation functional [12] knowing that this functional is of a sufficient quality for computational study on carbocation formation [13]. Kohn–Sham orbitals were represented by linear combinations of atomic orbitals using the 6-31G(d, p) basis sets.

In order to achieve the precision required for thermochemical calculations, tight convergence criteria were imposed. The geometries of substrates, carbocations and radicals were optimised in gas-phase at 0 K. In some cases, where conformation of ethyl group gave imaginary frequencies, the ultra fine grid in the optimisation was used. For carbocations and their substrates, the restricted close shell formalism was used whereas for radicals and corresponding neutral compounds unrestricted open shell formalisms were applied. The vibration analysis was performed in order to verify complete optimisation and to obtain the zero point vibration corrections that are necessary for thermochemical calculations (298 K, 1 atm, ZPE scale factor equal to 1). In some cases (ethylbenzene, 2-ethylnaphthalene, 2-ethylpyrrole, 2-ethyltoluene, 2-ethylphenol and n-propylbenzene) the conformational analysis was carried out in order to confirm that geometries with ethyl group perpendicular or near perpendicular to aromatic ring are indeed the ground states. In the case of carbocations and radicals of 2-ethyl compounds, both *E* and *Z* isomers were considered. As it was not apparent, which conformation is present in the enzyme active centre, the average value of energies for both conformers was used in the analysis. For *meta*- and *para*-substituted compounds as well as for those with substituents that can take two conformations (such as OH in plane of the ring) the conformation analysis was not performed as it was checked that the overall influence on the results of $\Delta\Delta G$ lies below computational error (i.e. less than 0.5 kJ/mol).

Changes in Gibbs free energy ΔG^{298} of hydride or hydrogen atom subtraction leading to carbocation or radical formation, respectively, were computed for all compounds. The ΔG values were obtained as a difference of free energy between products (carbocation and hydride, resp. radical and hydrogen atom) and substrates (neutral compound).

In order to compare the changes caused by the modified structures of substrate analogues, the respective ΔG values for ethylbenzene conversion were deducted from every value for substrate analogs, giving respectively, $\Delta\Delta G^{\text{carbocation}}$ and $\Delta\Delta G^{\text{radical}}$ values. Therefore, negative $\Delta\Delta G$ values indicate relative stabilization of the assumed intermediate (transition state) by the substituent, while positive $\Delta\Delta G$ values suggest relative destabilization of the assumed intermediate.

2.3. Validation of calculations

The thermochemical calculations were validated by comparison of the obtained thermodynamic parameters with literature data as far as available. The calculated values for methyl, ethyl, primary and secondary propyl, *tert*-butyl and benzyl radicals as well as for the corresponding carbocations were compared with changes of enthalpy (ΔH^{298}) taken from the literature [14].

The calculated reaction descriptors $\Delta\Delta G^{\text{radical}}$ and $\Delta\Delta G^{\text{carbocation}}$ were shown to behave in a similar manner as experiment-based QSAR descriptors such as the radical-term E_r [15,16] and the Hammett-constant σ^+ [9]. As the substitutes with available E_r are sparse and different from that studied with EBDH, additional calculations were conducted yielding dataset comprised of both experimentally tested substrates and additional compounds that were included to broaden the range of the assessed experiment-based descriptors. In all cases the ethylbenzene was used as a molecular core, i.e. E_r for 4-Cl was compared with $\Delta\Delta G^{\text{radical}}$ for 4-chloroethylbenzene while 4-CN substituent was coupled with $\Delta\Delta G^{\text{radical}}$ for 4-cyanoethylbenzene.

Table 1
Enthalpy changes (298 K, 1 atm) for formation of radicals and carbocations [14]

Compound	Radical (kJ/mol)		Carbocation (kJ/mol)	
	ΔH^{cal}	ΔH^{exp}	ΔH^{cal}	ΔH^{exp}
Methane	442	435	1386	1394
Ethane	422	410	1201	1256
Primary *n*-propene	423	410		
Secondary *n*-propene	405	398	1102	1160
Isobutane	392	381	1031	1097
Toluene	372	356	1044	1105

2.4. Correlation analysis

Correlation analysis was performed by the program Statistica 7.1 (Statsoft). The QSAR model describing the reaction rates of 21 com-

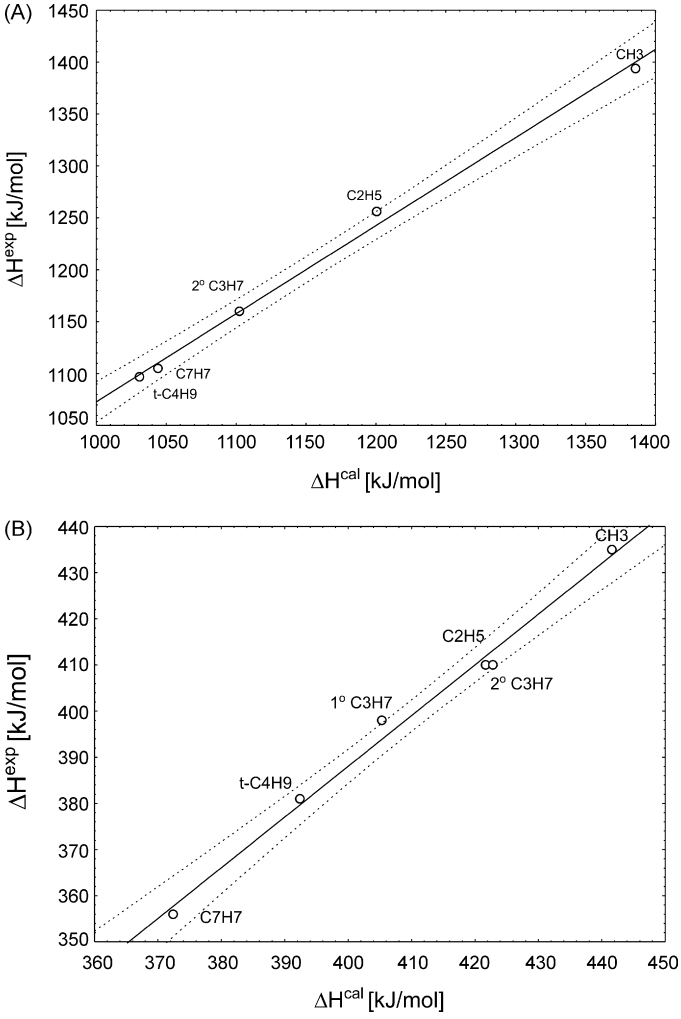

Fig. 4. Correlation plot of calculated (ΔH^{cal}) and experimental (ΔH^{exp}) changes of enthalpy upon: (A) carbocation formation ($R^2 = 0.9962$; $R = 0.9981$; $p = 0.00010$; $\Delta H^{\text{exp}} = 224.4146 + 0.8484 \times \Delta H^{\text{cal}}$); (B) radical formation ($R^2 = 0.9902$; $R = 0.9951$; $p = 0.00004$; $\Delta H^{\text{exp}} = -51.426 + 1.0987 \times \Delta H^{\text{cal}}$). The dashed lines depict 95% confidence level.

Table 2
Substrate spectrum of EBDH

Compound	Log k_{cat}	MR	Carbocation (kJ/mol)			Free radical (kJ/mol)		
			$\Delta\Delta G$	$\Delta\Delta GZ$	$\Delta\Delta GE$	$\Delta\Delta G$	$\Delta\Delta GZ$	$\Delta\Delta GE$
Ethylbenzene	2.00	37.74	0.00			0.00		
n-Propylobenzene	1.18	42.26	−3.94			1.13		
4-Ethyltoluene	1.45	43.12	−29.19			−2.32		
3-Ethyltoluene	1.00	43.12	−6.57			3.09		
2-Ethyltoluene	0.58	43.12	−10.48	−4.77	−16.20	3.27	8.63	−2.08
1,4-Diethylbenzene	1.54	47.63	−29.11			−2.58		
4-Ethylbiphenhyl	1.47	60.92	−47.13			−7.34		
2-Ethylnaphtalene	0.97	51.35	−36.82	−38.73	−34.91	−10.09	−12.25	−7.92
4-Ethylphenol	2.40	40.47	−46.60			−2.38		
3-Ethylphenol	1.28	40.47	−1.42			−1.19		
2-Ethylphenol	1.74	40.47	−31.55	−29.41	−33.70	2.46	6.19	−1.28
4-Ethylresorcinol	2.06	44.99	−70.46	−68.69	−72.24	1.84	5.64	−1.97
4-Propylphenol	2.26	46.87	−48.50			−3.47		
4-Ethylaniline	2.11	38.87	−96.73			−4.63		
2-Ethylanilne	1.96	46.34	−62.96	−59.45	−66.47	2.89	8.62	−2.85
4-Fluorethylbenzene	1.18	46.87	−3.20			−0.37		
4-Ethylanisol	1.36	19.88	−60.10			−2.28		
2-Ethylfuran	2.12	27.00	−38.13	−40.16	−36.10	−15.73	−16.62	−14.83
2-Ethylpyrrole	2.37	19.88	−73.94	−74.10	−73.77	−12.59	−10.67	−14.51
2-Ethylthiophene	2.38	27.51	−26.86	−28.75	−24.97	−17.22	−18.96	−15.47
3-Ethylpyridine	1.20	43.20	32.77			−1.19	−0.34	−0.34

Reactivity is provided as a logarithm of relative k_{cat} (ethylbenzene 100%). The compounds bulkiness is described by molecular refractivity (MR). The gas-phase changes of Gibbs free energies of carbocation and radical formation are presented as relative $\Delta\Delta G$ values. The ΔG^{298} for ethylbenzene is 1056 kJ/mol for carbocation and 321 kJ/mol for free radical formation. For *ortho*-substituted compounds $\Delta\Delta G$ is an average value of results obtained for *Z* and *E* conformations.

pounds was obtained by means of stepwise regression. Electronic effects were described by relative Gibbs free energy of carbocation formation ($\Delta\Delta G^{carbocation}$), while steric effects were described by molecular refractivity (MR) parameters that were calculated by the Cerius^2 program [17].

3. Results and discussion

3.1. Validation of calculations

In order to check if calculated thermochemical values correspond with those obtained experimentally, additional calculations were carried out for simple hydrocarbons. As only enthalpy changes were available for these compounds, the comparison was based on ΔH instead of ΔG. However, the computed entropic terms were almost constant for all investigated alkylaromatic and alkylheterocylic compounds (average ΔS values for carbocations 100 J mol^{-1} K^{-1}, and for radicals 122 J mol^{-1} K^{-1}), resulting in very high correlations of ΔH and ΔG values (R^2 = 0.9991 and 0.9190 for carbocations and radicals, respectively). Therefore, the validation of the ΔH values was taken as proof for the changes of Gibbs free energies. The results of calculations are presented in Table 1 and Fig. 4.

It is found that the computed ΔH values of radical formation correlate with the experimental ones with a R^2 = 0.9902 and the calculation method overestimates values of ΔH by 2–5%. A similar correlation is attained for carbocation formation (R^2 = 0.9962), whereas the ΔH values are underestimated by less than 6%. As in both cases these tendencies are systematic and linear and therefore they can be easily corrected from the regression equations (see Fig. 4).

3.2. Kinetic measurements

Our previous [8] and current studies show that EBDH exhibits activity with 21 substrates that can be divided into three groups, namely (i) non-activated hydrocarbons (2-, 3- and 4-ethyltoluene, 1,4-diethylbenzene, *n*-propylbenzene, 2-ethylnaphtalene and 4-ethylbiphenyl), (ii) hydrocarbons with non-carbon substituents in the aromatic ring (2-,3-,4-ethylphenol, 4-ethylresorcinol, 4-propylphenol, 2- and 4-ethylaniline, 4-ethylanisol, 4-fluoroethylbenzene) and (iii) heteroaromatic com-

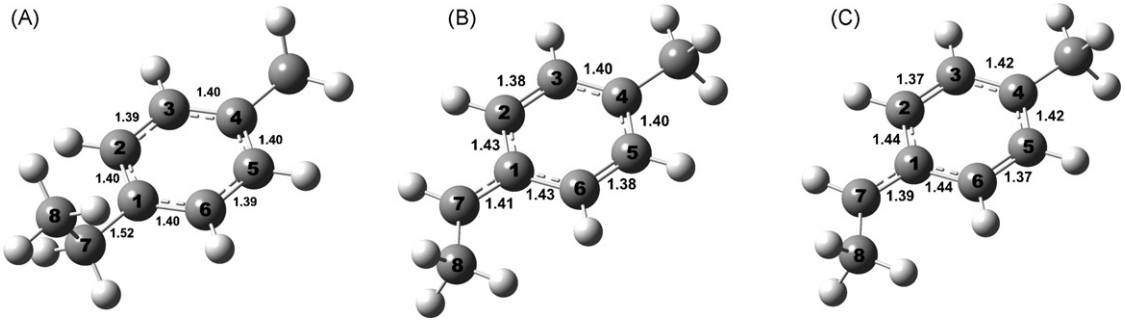

Fig. 5. The average geometry of *para*-substituted ethylbenzene derivates: (A) neutral compound; (B) radical ion; (C) carbocation. The dihedral angle between atoms No. 6–1–7–8 is 90° in the neutral molecule and 0° in carbocations and free radicals. The mean C1–C7 bond length is contracted from 1.52 Å in the neutral molecule to 1.41 Å in the free radical, and to 1.39 Å in the carbocation. Also the ring is deformed: the bonds between C2 and C3 and C5 and C6 are shortened from the mean value of 1.39–1.38 Å (free radical), resp. 1.37 Å (carbocation).

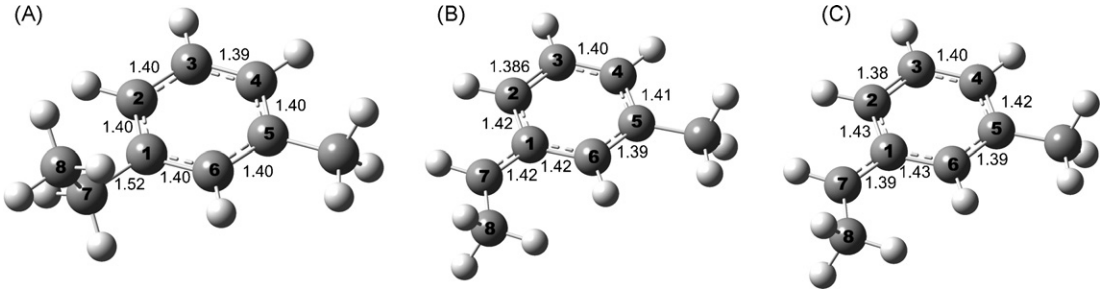

Fig. 6. The average geometry of *meta*-substituted ethylbenzene derivates: (A) neutral compound; (B) radical ion; (C) carbocation. The mean dihedral angle between atoms No 6–1–7–8 is 87° for neutral molecule and 0° for carbocations and free radicals. The mean C1–C7 bond is contracted from 1.52 Å in neutral form to 1.42 Å in free radical, and to 1.39 Å in carbocation. Also the ring is deformed: bond C2–C3 shortens from the mean value of 1.40 Å in neutral compound to 1.386 Å for free radical and 1.38 Å for carbocation, bond C5–C6 shortens from 1.40 to 1.39 Å, while the rest of ring bonds gets elongated (C1–C2 and C1–C6 from 1.40 to 1.42 Å in radicals and 1.43 Å in carbocations; bond C4–C5 elongates from 1.40 Å to 1.41 Å in radicals and 1.42 Å in carbocations).

pounds (2-,3-,4-ethylpyridine, 2-ethylpyrrole, 2-ethylfuran, 2-ethylthiophene). The relative k_{cat} spans two orders of magnitude from the worst substrate, 2-ethyltoluene ($\log k_{cat} = 0.58$) up to the best one, 4-ethylphenol ($\log k_{cat} = 2.4$). The investigation of their reactivity in reaction catalyzed by EBDH yields a list of kinetic constants that are collected in Table 2.

3.3. Geometries and energetics of neutral, radical and carbocation compounds

The optimisation of neutral substrates indicates that in the ground state the ethyl groups tend to be perpendicular to the plane of aromatic or heterocyclic ring. The biggest deviations from 90° dihedral angle are experienced for compounds with interacting *ortho* substituents such as 2-ethylaniline (74°) or heteroatoms, such as 2-ethylfuran (63°).

3.3.1. Para-substituted ethylbenzene derivates

In global energetic minimum the *para*-substituted ethylbenzene derivates in their neutral form exhibit a perpendicular conformation of the ethyl group towards the aromatic ring (dihedral 6–1–7–8 equal to 90°) and a symmetric ring structure with C–C bond lengths between 1.39 and 1.40 Å. Both radicals and carbocations have a planar conformation of the ethyl group with a dihedral angle between the ring and the ethyl group equal to zero (Fig. 5). However, there are some noticeable structural differences between the free radicals and carbocations. The C–C bonds linking the ethyl groups with the ring as well as the ring bonds between atoms C2 and C3 or C5 and C6 are more shortened in carbocations than in radicals (Fig. 5).

3.3.2. Meta-substituted ethylbenzene derivates

The neutral *meta*-substituted ethylbenzene derivates have almost perpendicular conformation of the ethyl group (mean dihedral 6–1–7–8 equals 87°) and even C–C ring bond length (1.40 Å) with the exception of slightly shorter bond between C3 and C4 (1.39 Å). In case of both radicals and carbocations the ethyl group is present in a planar conformation and some distortion of bond lengths occurs (see Fig. 6). The steric interaction between ethyl group and *meta* substituent is very small (for example in case of one of test compound, 1,3-diethylbenzene *Z* conformer has ΔG lower than *E* isomer by 0.42 kJ/mol). As a result, the overall energetics of carbocation or radical formation seems to be insensitive to the conformation of ethyl group (*E* or *Z*). The difference in free enthalpy of formation between both conformers is in the range of 2 kJ/mol and lies within the calculation error. Therefore, only *Z* conformers are used in QSAR analysis.

3.3.3. Ortho-substituted ethylbenzene derivates

The neutral *ortho*-substituted ethylbenzene derivates have fairly perpendicular conformation of ethyl group (mean dihedral C6–C1–C7–C8 equals 80°) indicating electronic interaction between substituent and ethyl group (the biggest deviation from perpendicular conformation, 74°, appears for 2-ethylaniline). There are some additional deviations in C–C ring bond lengths from 1.40 Å with C1–C6 bond length being on average longer of 0.01 Å and bonds C3–C4 and C4–C5 being shorter by 0.01 Å (Fig. 7).

As a result of planar conformation of ethyl group for *ortho*-substituted compounds there are two possible conformations (*E* and *Z*: see Fig. 8) where close molecular interaction can take place. Significant difference in energetic between two conformers was

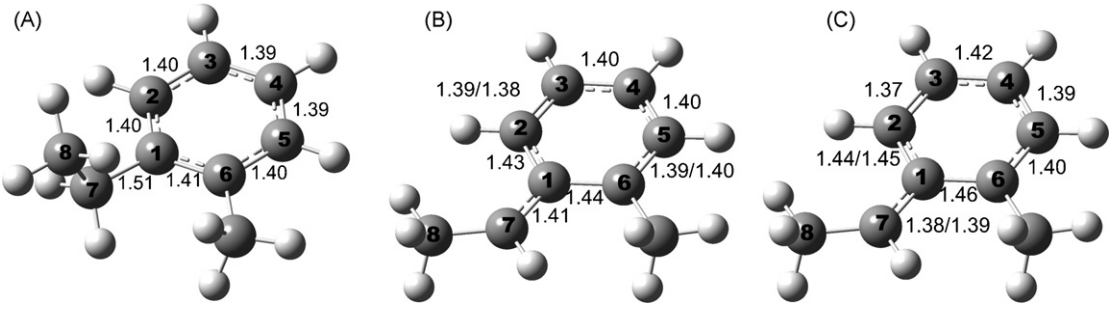

Fig. 7. The average geometry of *ortho*-substituted ethylbenzene derivates: (A) neutral compound; (B) radical ion; (C) carbocation. Bond lengths are provided in Å for *E*/*Z* conformations. The mean dihedral angle between atoms No 6–1–7–8 is 80° for neutral molecule and 0° for carbocations and free radicals. The mean C1–C7 bond is contracted from 1.52 Å in neutral form to 1.41 Å in free radical, and to 1.38/1.39 Å in carbocation. Also the ring is deformed: mean length of bonds C1–C6/C1–C2 elongates from 1.41/1.40 to 1.43/1.44 Å for radicals and from 1.44/1.45 to1.46 Å for carbocations. Bonds C3–C4 and C4–C5 elongates from 1.39 to 1.40 Å in radicals while for carbocations only mean C3–C4 bond length increases to 1.42 Å. Bonds C2–C3 and C5–C6 contract by 0.01–0.03 Å.

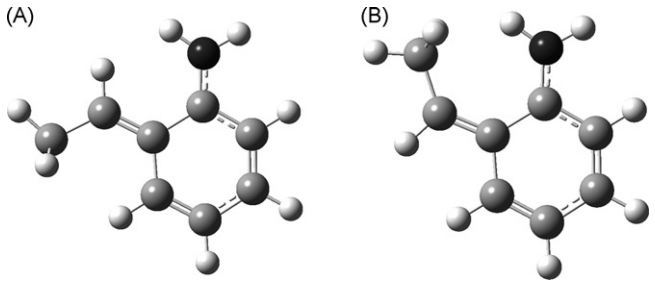

Fig. 8. Two possible conformations of *ortho*-substituted radical/carbocation ion on the example of 2-ethylaniline carbocation ((2-aminophenyl)ethylium) in (A) *E* conformation and (B) *Z* conformation.

a basis for performing calculations for both forms. The ring distortion is similar as seen for *para*-substituted compounds, i.e. generally there is elongation of the C1–C2, C1–C6, C3–C4 and C4–C5 bonds and contraction of C2–C3 and C5–C6 bonds. However, the geometric changes are influenced by the conformation of the ethyl group. In *Z* conformers, the C1–C2 and C1–C6 bonds are elongated coming most probably from steric repulsion (Fig. 8).

In most cases the *Z* conformations for radicals have higher energy, due to the steric hindrance introduced by *ortho* substituents (see Table 2). The Gibbs free energy difference between both conformations (*Z* minus *E*) ranges between 7.5 kJ/mol in case of the 2-ethylphenol and 4-ethylresorcinol radical, up to 11.5 kJ/mol for the 2-ethylaniline radical. However, for 2-ethyl heterocyclic compounds the differences are much smaller (below 4 kJ/mol). In case of 2-ethylthiophene and 2-ethylfuran, the *Z* conformation turns out to be more preferable (for both radicals and carbocations).

Similarly, for carbocations the *Z* conformation turns out to be less stable (*Z* minus *E*: 2-ethyltoluene 11 kJ/mol, 2-ethylaniline 7 kJ/mol, 2-ethylphenol 4.3 kJ/mol). Interestingly, the heterocycle carbocation compounds have *Z* conformation more stable or both conformers are characterized by energies of almost equal values (for e.g. 0.3 kJ/mol difference for 2-ethylpyrrole).

In enzyme active centre the overall energetics (and consequently kinetics) is influenced not only by intermolecular interactions but also by close contacts between substituents and molybdenum cofactor and amino acid residues. Therefore, it is impossible to discern which conformation would be preferred and, as a result, the average value of both $\Delta\Delta G$s for *E* and *Z* conformers is used for further analysis.

3.4. Free energies of formation—correlation with σ^+ and E_r

The $\Delta\Delta G$ descriptors are very useful as parameters for QSAR because they can be calculated for almost any organic compound. Moreover, in case of ethylbenzene derivates the obtained values represent not only the effect introduced by the substituent, but the whole existing interactions (including the influence of the site of the reaction at the ethyl or propyl side chain) on overall energetics. The calculated $\Delta\Delta G$ for all known EBDH substrates are provided in Table 2.

For additional validation of the obtained results, the correlation with widely accepted QSAR descriptors such as Hammet σ^+ and radical Yamamoto–Otsu E_r constant was investigated. It was necessary to check the correlation of σ^+ and E_r with both $\Delta\Delta G^{carbocation}$ and $\Delta\Delta G^{radical}$ for the same dataset. However, radical constants were available only for a dozen or so compounds, most of which do not overlap with the EBDH substrate spectrum. On the other hand, it was necessary for a useful validation to include a substantial number of the substituents used in $\Delta\Delta G$ examination into the analysis

Table 3
The control dataset used in correlation analysis

Compound	σ^+	$\Delta\Delta G^{carbocation}$ [kJ/mol]	E_r	$\Delta\Delta G^{radical}$ [kJ/mol]
Substrates				
Ethylbenzene	0	0	0	0
4-Ethyltoluene	−0.31	−29.19	0.03	−2.32
3-Ethyltoluene	−0.07	−6.57	0.02	3.09
1,4-Diethylbenzene[a]	−0.30	−29.11	0.01	−2.58
4-Ethylbiphenhyl	−0.18	−47.13	0.31	−7.34
4-Ethylphenol	−0.92	−46.60	0.17	−2.38
4-Ethylanisol	−0.78	−60.10	0.11	−2.28
4-Fluorethylbenzene[a]	−0.07	−3.20	−0.04	−0.37
Supplementary compounds				
3-Ethylanisol	0.12	−14.28	0.01	−1.37
4-Chlorethylbenzene	0.11	6.01	0.10	−1.69
4-Bromoethylbenzene	0.15	2.49	0.12	−3.10
4-Ethyl-*N*,*N*-dimethylaniline	−1.70	−120.21	0.24	−5.63
4-Cyanoethylbenze	0.66	49.04	0.24	−8.19

The gas-phase changes of Gibbs free energies for carbocation and radical formation are presented as relative $\Delta\Delta G$ values. The ΔG^{298} for ethylbenzene is 1056 kJ/mol for carbocation and 321 kJ/mol for free radical formation. The σ^+ and E_r values are taken from Hansch and Leo [18].

[a] Value calculated from Wayner and Arnold σ [19].

and to compose a validation data set from substituents with different values of E_r and Hammet σ^+. Thus, a dataset containing 13 compounds was assembled that contained eight EBDH substrates and five additional compounds (Table 3). This approach provided compounds with known values of Hammet σ^+ ranging from −1.70 to 0.66 and E_r values from −0.04 to 0.31.

Correlation analysis reveals that the calculated $\Delta\Delta G^{carbocation}$ values correlate strongly with Hammett σ^+ values ($R^2 = 0.9092$, $p = 5 \times 10^{-8}$, Fig. 9) and $\Delta\Delta G^{radical}$ values correlate, albeit with lesser strength, with Yamamoto–Otsu E_r values ($R^2 = 0.7041$, $p = 0.0003$, see Fig. 10). However, there are no statistically significant correlations of $\Delta\Delta G^{carbocation}$ values with E_r ($R^2 = 0.0914$; $p = 0.3154$) and $\Delta\Delta G^{radical}$ values with σ^+ ($R^2 = 0.0036$; $p = 0.8448$). Finally, the $\Delta\Delta G^{radical}$ and $\Delta\Delta G^{carbocation}$ values do not correlate neither in the control dataset nor in the real substrates dataset ($R^2 < 0.07$; $p > 0.25$). Therefore, the $\Delta\Delta G^{carbocation}$ values seem to describe properly the substituent-derived stabilization effect for carbocations, whereas the $\Delta\Delta G^{radical}$ values for radicals.

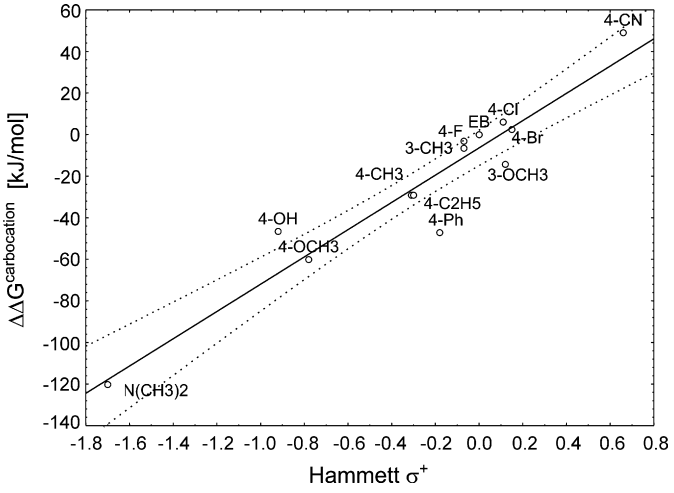

Fig. 9. The correlation plot between Hammett σ^+ and $\Delta\Delta G^{carbocation}$ ($R^2 = 0.9092$, $R = 0.9535$, $p = 5 \times 10^{-7}$). Dotted line depicts 95% confidence area.

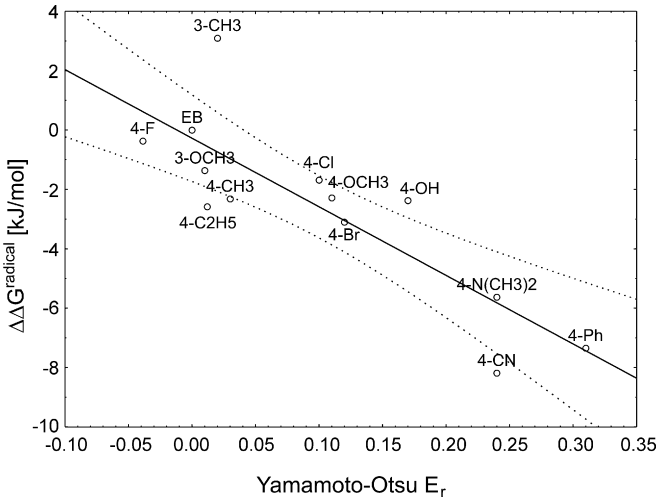

Fig. 10. The correlation plot between Yamamoto–Otsu E_r and $\Delta\Delta G^{radical}$ ($R^2 = 0.7041$, $R = 0.8391$, $p = 3 \times 10^{-4}$). Dotted line depicts 95% confidence area.

3.5. Correlation of $\Delta\Delta G$ with kinetic parameters

A single electronic parameter, such as $\Delta\Delta G$, was not expected to describe the whole variety of reactivity of the enzyme reaction. It was shown previously, that model containing more than one parameter must be used for a description of reactivity of all substrates [7,8]. However, the comparison of correlation between reaction rates and a single parameter provides a direct insight into the data distribution, which allows graphical validation of statistical correlation indices. Since above it was proven that the methodology of $\Delta\Delta G$ calculation was uniform for both radicals and carbocations, it was assumed that both $\Delta\Delta G^{carbocation}$ and $\Delta\Delta G^{radical}$ values can be compared and treated as valid descriptors of carbocation and radical ethylbenzene activation, respectively.

The correlation of $\log k_{cat}$ with both types of the $\Delta\Delta G$s yields the same, medium strength correlation: for carbocation $R = -0.5686$ and for radicals $R = -0.4398$. However, one should remember that for the proper analysis the graphical representation of the correlations in the form of scatter plots is necessary, because these plots show how the reaction rate ($\log k_{cat}$) changes with an increase of either $\Delta\Delta G^{radical}$ or $\Delta\Delta G^{carbocation}$. In the scatter plots for radicals (Fig. 11B) the points are scattered in a random way and the regression line does not reveal a real trend. Meanwhile, in case of carbocations there is a clearer correlation between more negative $\Delta\Delta G$s and higher reaction rates (the regression line has negative slope and points, though scattered aggregate along the line). The plot shows that lowering the energy of hypothetic carbocation intermediate would result in acceleration of the reaction kinetics.

The insight provided by the above-mentioned correlation analysis permits us to propose carbocation type transition state as a rate-limiting step that is observed in the experimental test [8]. Because values of Gibbs free energy do not take into account bulkiness of the substrate the molecular refractivity (MR) is added to the analysis. This allows formulation of an equation, which is a slight extension of that given in a previous paper (based on 21 substrates instead of 20):

$$\log k_{cat} = -0.70(\pm 0.15)\,\Delta\Delta G^{carbocation} - 0.56(\pm 0.15)\,MR + 2.47$$

The obtained equation predicts the experimental results with $R^2 = 0.61$, which is a significant improve over single parameter correlation ($R^2 = 0.3233$), and allows description of the reactivity for all tested substrates. The quality of prediction can be assessed from correlation plot (Fig. 12) that provides both $\log k_{cat}$ values

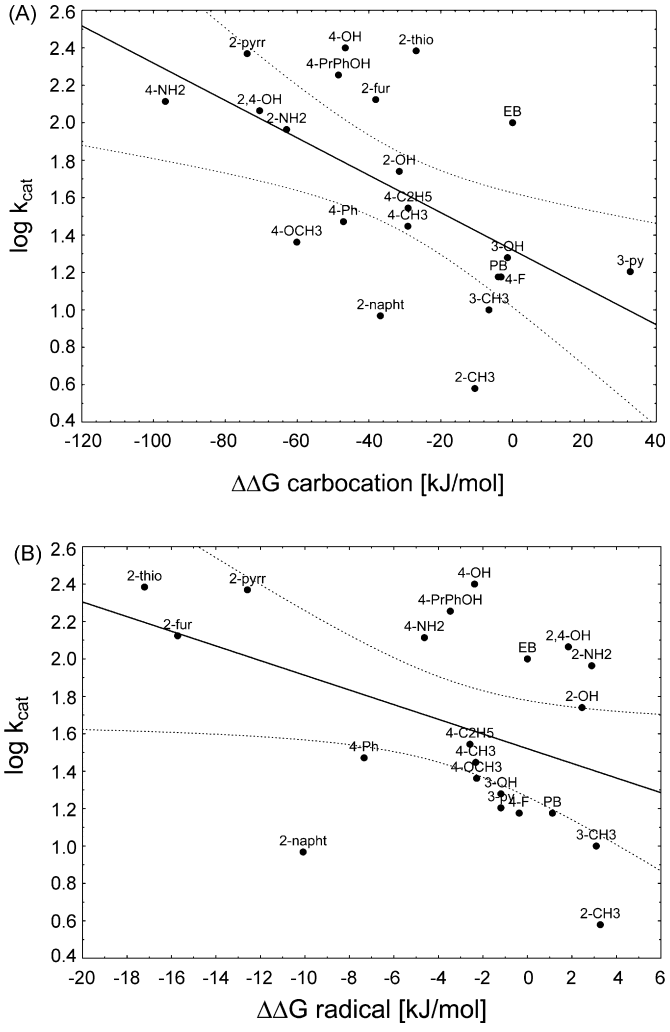

Fig. 11. Correlation plots of logarithm of kinetic constant ($\log k_{cat}$) with: (A) $\Delta\Delta G^{carbocation}$ ($R^2 = 0.3233$; $R = -0.5686$; $p = 0.0071$) and (B) $\Delta\Delta G^{radical}$ ($R^2 = 0.1935$; $R = -0.4398$; $p = 0.0460$). Although correlation statistics are in the same range in both cases the analysis of graphical point scatter for radicals reveals no linear correlation. The obtained trend seems to be coincidental. Meanwhile, the carbocation points scatter clearly along the regression line.

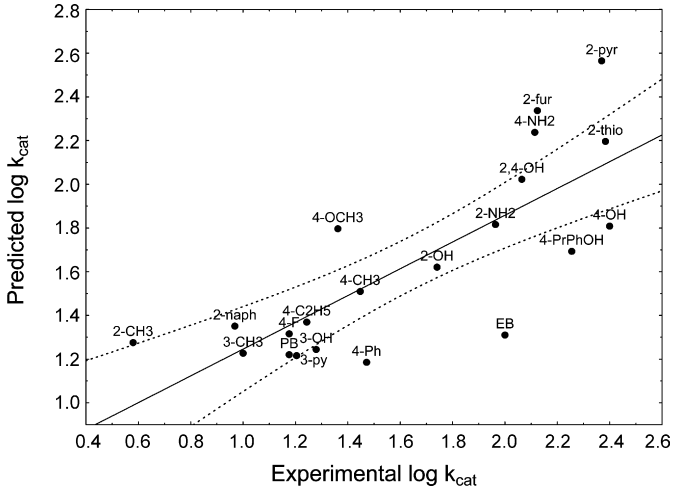

Fig. 12. Correlation of predicted relative k_{cat} with experimental values in regression model ($R^2 = 0.6126$; $R = 0.7827$; $p = 0.00003$). Labels describe the localization of substituents with respect to ethylbenzene core (e.g. 3-OH states for 3-ethylphenol). The dashed lines depict 95% confidence level.

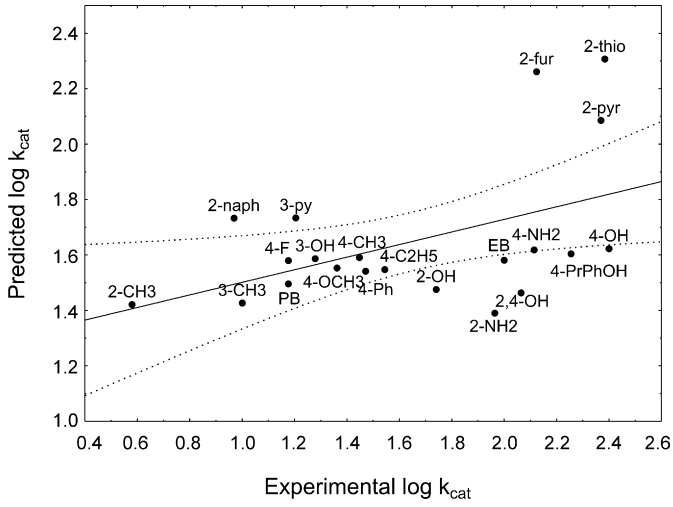

Fig. 13. Correlation of predicted relative k_{cat} with experimental values in regression model with $\Delta\Delta G^{radical}$ instead of $\Delta\Delta G^{carbocation}$ ($R^2 = 0.2271$; $R = 0.4766$; $p = 0.0289$). Labels describe the localization of substituents with respect to ethylbenzene core (e.g. 3-OH states for 3-ethylphenol). The dashed lines depict 95% confidence level.

from experiment and that calculated from the model. The negative coefficients of the $\Delta\Delta G^{carbocation}$ values indicate that stabilization of carbocation intermediates (i.e. lowering the ΔG values, more negative values of $\Delta\Delta G$) accelerates reaction rate. The negative coefficient of MR shows that steric hindrance decreases the reaction rate.

The carbocation like TS hypothesis can be further supported by the comparison of the above equation with the one, where $\Delta\Delta G^{carbocation}$ is replaced by $\Delta\Delta G^{radical}$. The overall regression statistics indicates that such an equation is no longer statistically significant (p levels for both parameters above 0.05) while the R^2 of a scatter plot between experimental and predicted $\log k_{cat}$ has $R^2 = 0.2271$ (Fig. 13) which shows basically no improvement over correlation solely with $\Delta\Delta G^{radical}$ ($R^2 = 0.1935$). Moreover, one can see from the scatter plot presented in Fig. 13 that there is no correlation between experimental values and those predicted by regression model (horizontal distribution of points).

4. Discussion

Having good quantum chemical parameter describing stabilization of radical or carbocation transition state one would aspire to identify chemical mechanism present in reactions catalyzed by EBDH. Such a hope might be indeed reasonable in case of simpler chemical systems. However, it would be too daring to claim that it is possible to discern the electronic structure of the transition state during the enzymatic reaction based solely on the computation results performed for isolated organic molecules in gas-phase. The carbocation intermediate seems to be (on average) more probable than a free radical intermediate due to: (i) more systematic distribution of scatter point in correlation plot and (the lowered free enthalpy of carbocation formation by substituents, which stabilizes positive charges, correlates with increased reaction rates), (ii) the fact that $\Delta\Delta G^{carbocation}$ could be used in regression model.

The situation in the real catalytic site might be however, a bit more complex. For example, the reaction might either proceed via one two-electron oxidation or two one-electron oxidations, the latter involving a radical intermediate. Moreover, it should be realized that in the transition state the C···H bond is weakened while H···O–Mo is not yet entirely formed which corresponds to the maximum of potential energy on the reaction pathway. Therefore, both spin density and charge may be accumulated in TS1 on the hydrocarbon, which would cause some carbocation-like stabilization of a radical intermediate. Finally, in case of a mixed radical-carbocation mechanism (with radical TS1 and carbocation TS2) the actual rate-limiting step might change because of uneven substituent stabilization effects of radical and carbocation formation. In such a situation the reaction rate of some EBDH substrates may be limited by radical C–H cleavage and other processes caused by carbocation formation or OH rebound. Therefore, even if the rate-limiting step seems to involve carbocation formation on average, in some cases the energy of carbocation TS might be lowered to such extent that the radical barrier starts to limit the reaction rate. This might be the case with 4-ethylanisole, which although having very negative $\Delta\Delta G$ for carbocation formation (−60.10 kJ/mol), has relatively small $\Delta\Delta G$ for radical formation (−2.28 kJ/mol) and is converted at rather low rate.

In order to elucidate this matter, quantum chemical modelling of the full reaction pathway with various substrates are conducted, so the obtained results can be compared with kinetic measurements and the electronic nature of postulated transition states can be carefully analyzed. This will be supplemented by isotope kinetic measurements with deuterated substrates, and quantum chemical calculation of $\Delta G^{\#}$ that will allow estimation of an isotope effect which should be higher in case of C–H cleavage and lower for OH rebound [20].

5. Conclusions

It is shown that gas-phase quantum chemical calculations can provide thermochemical data to be used as versatile QSAR descriptors. The calculated $\Delta\Delta G^{carbocation}$ values correlate strongly with Hammett σ^+ experimental values whereas the $\Delta\Delta G^{radical}$ values correlate with Yamamoto–Otsu E_r experimental values. The $\Delta\Delta G$ descriptors are very useful as parameters for QSAR because they can be calculated for almost any organic compound. The correlation analysis of experimental kinetic data and changes in gas-phase Gibbs free energies of formation for carbocation and radical intermediates elucidates the nature of the rate-limiting step in the reaction mechanism of ethylbenzene dehydrogenase. The application of $\Delta\Delta G^{carbocation}$ together with molecular refractivity MR allows fairly good prediction of substrate activity and suggests that carbocation-like TS is limiting in most of the analyzed cases.

The methodology presented in this paper, appears to be a plausible alternative to standard QSAR, especially in cases, when standard descriptors are not available for a set of compounds and different types of reaction mechanisms need to be validated. It seems that such analysis provides a systematic procedure for rationalization of chemical intuition in the research on mechanisms of chemical reactions.

Acknowledgments

This research has been supported by Polish Ministry of Science and Higher Education under grant KBN/SGI2800/PAN/037/2003 and Scientific Network EKO-KAT and by the Deutsche Forschungsgemeinschaft (He2190/4-1). Maciej Szaleniec acknowledges a PhD grant of Polish Academy of Sciences.

References

[1] R. Hille, Chem. Rev. 96 (1996) 2757–2816.
[2] H.A. Johnson, D.A. Pelletier, A.M. Spormann, J. Bacteriol. 183 (2001) 4536–4542.
[3] O. Kniemeyer, J. Heider, J. Biol. Chem. 276 (2001) 21381–21386.
[4] R. Rabus, M. Kube, A. Beck, F. Widdel, R. Reinhardt, Arch. Microbiol. 178 (2002) 506–516.

[5] J.P. Schur. Additive for improving the storage life of and/or stabilising microbially perishable products Canadian patents database, Patent document number 2294989, US Patent 7,108,879, September 19, 2006.
[6] I. Mohamad, R.W. Blocker, J. Arvizzigno, R. Muralidhara, Mixtures of optical isomers of styralyl alcohol or styralyl acetate, processes for preparing same and organoleptic uses thereof, US Patent 6,511,686, January 28, 2003.
[7] M. Szaleniec, M. Witko, R. Tadeusiewicz, J. Goclon, J. Comput. Aided Mol. Des. 20 (2006) 145–157.
[8] M. Szaleniec, C. Hagel, M. Menke, P. Nowak, M. Witko, J. Heider, Biochemistry 46 (2007) 7637–7646.
[9] Y. Okamoto, H.C. Brown, J. Org. Chem. 22 (1957) 485–494.
[10] C. Hansch, H. Gao, Chem. Rev. 97 (1997) 2995–3059.
[11] M.J. Frisch, G.W. Trucks, H.B. Schlegel, G.E. Scuseria, M.A. Robb, J.R. Cheeseman, J.A. Montgomery Jr., T. Vreven, K.N. Kudin, J.C. Burant, J.M. Millam, S.S. Iyengar, J. Tomasi, V. Barone, B. Mennucci, M. Cossi, G. Scalmani, N. Rega, G.A. Petersson, H. Nakatsuji, M. Hada, M. Ehara, K. Toyota, R. Fukuda, J. Hasegawa, M. Ishida, T. Nakajima, Y. Honda, O. Kitao, H. Nakai, M. Klene, X. Li, J.E. Knox, H.P. Hratchian, J.B. Cross, V. Bakken, C. Adamo, J. Jaramillo, R. Gomperts, R.E. Stratmann, O. Yazyev, A.J. Austin, R. Cammi, C. Pomelli, J.W. Ochterski, P.Y. Ayala, K. Morokuma, G.A. Voth, P. Salvador, J.J. Dannenberg, V.G. Zakrzewski, S. Dapprich, A.D. Daniels, M.C. Strain, O. Farkas, D.K. Malick, A.D. Rabuck, K. Raghavachari, J.B. Foresman, J.V. Ortiz, Q. Cui, A.G. Baboul, S. Clifford, J. Cioslowski, B.B. Stefanov, G. Liu, A. Liashenko, P. Piskorz, I. Komaromi, R.L. Martin, D.J. Fox, T. Keith, M.A. Al-Laham, C.Y. Peng, A. Nanayakkara, M. Challacombe, P.M.W. Gill, B. Johnson, W. Chen, M.W. Wong, C. Gonzalez, J.A. Pople, Gaussian 03, Revision D.01, Gaussian, Inc., Wallingford, CT, 2004.
[12] A.D. Becke, J. Chem. Phys. 98 (1993) 5648.
[13] M. Pittelkow, J.B. Christensen, T.I. Sølling, Org. Biomol. Chem. 3 (2005) 2441–2449.
[14] R.T. Morrison, R.N. Boyd, Organic Chemistry, 3rd ed., Allyn and Bacon, Inc., USA, Boston, 1996.
[15] Y. Yamamoto, T. Otsu, Chem. Ind. 787 (1967).
[16] C. Hansch, E. Kutter, A. Leo, J. Med. Chem. 12 (1969) 476–749.
[17] Accelrys Software, Inc., Cerius^2 Modeling Environment, Release 4. 8, Accelrys Software, Inc., San Diego, 2005.
[18] C. Hansch, A. Leo, Exploring QSAR, Fundamentals and Application in Chemistry and Biology, ACS Processional Reference Book, American Chemical Society, Washington, DC, 1995.
[19] D.D.M. Wayner, D.R. Arnold, Can. J. Chem. 43 (1978) 224.
[20] M. Szaleniec, M. Witko, J. Heider, Proceedings of Europacat VIII, Turku, Finland, 2007, pp. P6–P10.